Structure of colloidal glasses calculated by the molecular-dynamics method and measured by light scattering

I. Snook, W. van Megen, and P. Pusey
Department of Applied Physics, Royal Melbourne Institute of Technology, Melbourne, Victoria 3001, Australia
(Received 29 January 1990; revised manuscript received 13 September 1990)

Static structure factors $S(q)$ were measured by laser light scattering for very concentrated systems of spherical, near-monosized, sterically stabilized particles dispersed in nonpolar liquids. A range of systems with particle concentrations beyond that corresponding to the disorder to order transition configurations were found to have amorphous structures. As the particles were stabilized by means of very short chain polymers, these systems were thought to closely approximate the fundamentally important amorphous, hard-sphere system. Subsequent analysis of $S(q)$ carried out by means of data generated by the molecular-dynamics method for very concentrated, amorphous states of the hard-sphere system confirmed this interpretation. Thus we were able, by a combination of experiment and simulation, to give an extensive analysis and description of the structure of the amorphous state of a system of hard spheres. This study complements past work on the thermodynamic and transport properties of metastable, amorphous states of a system of hard spheres.

I. INTRODUCTION

Concentrated dispersions of small particles in liquids form the basic ingredients of many materials, such as paints, cosmetics, soils, and the presintered state of ceramics. Obviously, an understanding of, and the ability to control their properties, is of considerable technological value. For example, studies of ceramic processing suggest a strong correlation between the mechanical strength of the final product and the state of aggregation of the presintered dispersion.[1,2] Further, the economics of the sintering process are significantly improved by using dispersions at high volume fractions with particles as close to monodisperse as possible.[2] The ease with which a stable dispersion can be (osmotically) compressed depends on the range and strength of the forces between the particles and one way to achieve the large solids content, desirable in many applications, is by employing particles stabilized by very thin adsorbed polymer layers.[3] A "model" or laboratory prepared dispersion that meets this specification comprises near micron sized spherical polymethylmethacrylate (PMMA) particles (or "cores") stabilized by a chemically adsorbed layer of poly-12-hydroxystearic acid (PHSA) chains of approximately 10-nm thickness.[4] These particles can be prepared with very narrow particle size distribution and be dispersed in a variety of nonpolar liquids including liquid mixtures whose refractive index closely matches that of the particles. The resulting optically matched, nearly transparent dispersions are then suitable for light scattering studies.[5,6]

As the volume fraction ϕ of these dispersions is increased they display the transition from a fluidlike or disordered phase to the crystal phase similar to that expected for an atomic fluid.[5] The difference in the volume fractions of the coexisting crystalline and disordered phases is close to that known for the simple hard-sphere system; this is an indication of the very short range of repulsion forces between the particles. Laser light scattering has been applied to these dispersions to determine their static structure factors[7] as well as the coherent and incoherent dynamic structure factors.[8,9]

A particularly interesting and possibly useful characteristic of a dispersion of near micron sized particles is that the structural relaxation times τ as measured from the decay of the dynamic structure factors are many orders of magnitude greater than those for fluids of inert atoms.[7,8] For dispersions near the crystallization transition τ is typically of order 0.1 sec and lengthens appreciably with increasing ϕ. This characteristic not only permits a direct study of the metastable fluid state, but allows sufficiently rapid compression to metastable states for which τ exceeds any reasonable experimental time. The volume fraction ϕ_g around which τ increases abruptly by several orders of magnitude (to $\tau > 10^3$ sec) coincides almost perfectly with the macroscopically observed glass transition (GT), i.e., above ϕ_g no homogeneously nucleated crystallization is observed.[8] By contrast compression (or cooling) of simple atomic fluids sufficiently rapidly to bypass crystallization is presently not possible by experimental means.[10] However, compression rates which exceed structural relaxation in atomic liquids can be achieved in computer simulation.[10]

A comparison of the particle dynamics of the PMMA dispersions, discussed above, with those of simple atomic fluids, in the vicinity of the GT as predicted by computer simulation and theory, will be discussed elsewhere. In this paper we compare the (static) structure factors obtained by molecular-dynamics computer simulations on dense (metastable) hard-sphere fluids with those measured by light scattering on concentrated PMMA dispersions.

II. EXPERIMENTAL DETAILS

The synthesis of the PMMA latex particles and the preparation of transparent dispersions of a specified volume fraction have been detailed in previous publications.[4,6,9] For the present study the hydrodynamic particle radius, as measured by dynamic light scattering, is 305±6 nm with a polydispersity (given by the ratio of the width of the particle size distribution to the average radius) of about 5%. The complete phase behavior of this dispersion, which displays the transitions from disordered to crystalline to glass states with increasing volume fraction, has been discussed in earlier work.[4,7] There the volume fraction, obtained by weight analysis of the dispersion, at which crystallization commences was equated with the freezing volume fraction $\phi_F=0.494$ of the hard-sphere system.[11] An indication of the short range of the repulsion between the particles, which justifies the use of the hard-sphere model, is provided by the extremely sudden and steeply increasing osmotic pressure with increasing ϕ[3]. Further justification is provided by the fact that the observed (effective hard-sphere) volume fraction at which the crystalline dispersion melts[5,7] is only marginally below the melting volume fraction of 0.545 predicted by computer simulations for a system of hard spheres.[11] It is relevant that computer simulation studies indicate considerable sensitivity of the quantity $(\phi_m-\phi_F)/\phi_F$ to the range (of softness) of the interparticle potential.[12] Other characteristics of this dispersion significant to this paper are that the glass transition occurs at a volume fraction $\phi_g=0.58$ and that in the range $\phi_F<\phi<\phi_g$ any crystals are easily disrupted ("shear melted") to a metastable disordered state by gently agitating the samples.[7] Except for $\phi=\phi_m$ recrystallization takes place sufficiently slowly to allow light scattering measurements of the metastable states.[7,9]

For a dispersion of identical spheres the average scattered intensity is

$$I(q)=cP(q)S(q)\ , \tag{1}$$

where the scattering vector is

$$q=\frac{4\pi n}{\lambda}\sin\theta/2\ . \tag{2}$$

Here n is the refractive index of the dispersion, λ the wavelength of the (laser) radiation, and θ the scattering angle. c is a constant proportional to the particle concentration, $P(q)$ is the single-particle scattering function, and $S(q)$ is the structure factor. For an isotropic dispersion

$$S(q)=1+\frac{6\phi}{25}\int_0^\infty [g(r)-1]\frac{\sin qr}{qr}r^2dr\ , \tag{3}$$

where $g(r)$ is the radial distribution function. At infinite dilution, where the spatial correlation between the particles is absent, $g(r)=1$ and $S(q)=1$, so that the scattered intensity becomes

$$I_0(q)=C'P(q)\ . \tag{4}$$

Since the refractive indices of the particles and the supporting liquid are quite closely matched in order to provide transparent samples and minimize multiple scattering, $P(q)$ is quite sensitive to small variations in the refractive index of the liquid. To ensure that $P(q)$ is consistent in the measurements of both $I(q)$ and $I_0(q)$, the latter was measured on a dilute sample obtained as follows.[7] A sample on which $I(q)$ was measured was centrifuged until the particles formed a compact sediment. Gentle agitation caused the release of a small number of particles into the clear supernatant providing a dilute dispersion for the measurement of $I_0(q)$. Both $I(q)$ and $I_0(q)$ were also corrected for the scattering from the pure liquid. Un-normalized structure factors can then be obtained from the ratio of Eqs. (1) and (4).

Normalization was effected by adjusting the measured structure factor for the fluid phase coexisting with the crystalline phase (i.e., of $\phi=\phi_F$) with the known structure factor of the hard-sphere fluid at freezing to give a best fit with theory, as judged by eye. We should emphasize that these experimental structure factors are somewhat preliminary in nature and may be subject to significant, as yet unquantified, experimental errors. These uncertain-

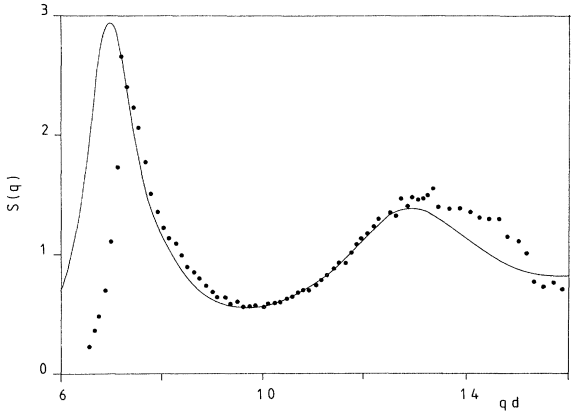

FIG. 1. $S(q)$ for a hard-sphere fluid at *coexistence* with a hard-sphere solid (——), and the corresponding result for colloidal suspension under the same conditions (●).

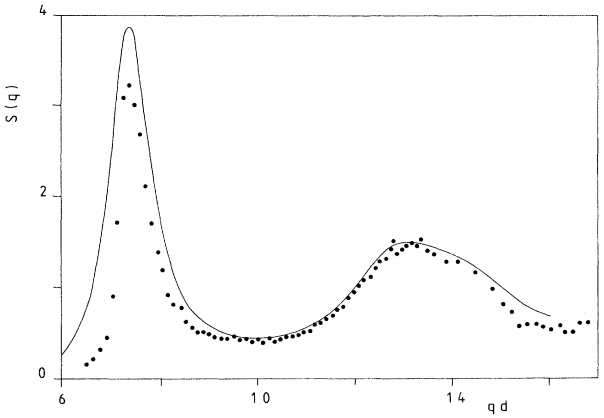

FIG. 2. Same as for Fig. 1 but $\rho^*=1.10$.

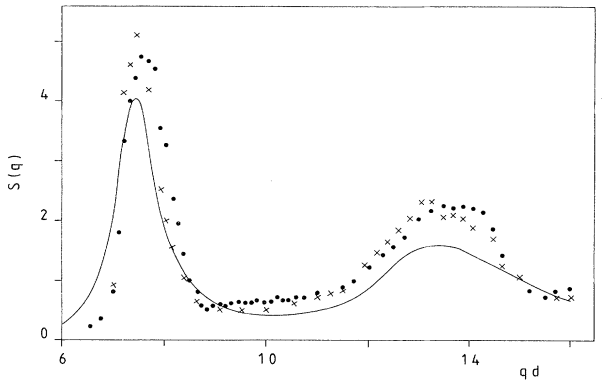

FIG. 3. Same as for Fig. 1 but $\rho^* = 1.14$, showing results for the spun-down sample (●) and the sample slowly tumbled and allowed to equilibrate (×).

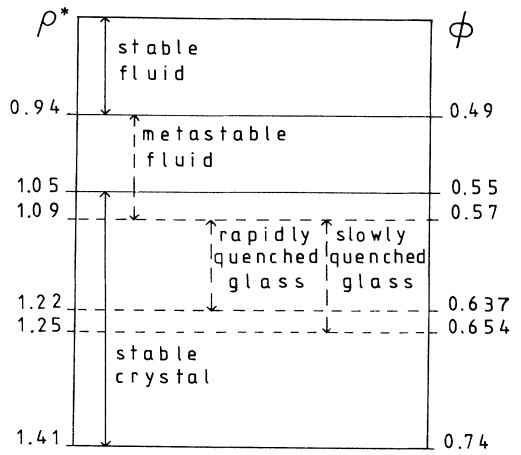

FIG. 5. Schematic phase diagram of the hard-sphere system.

ties are expected to be most pronounced in the region of the minimum in $P(q)$ which, for optically homogeneous hard spheres, roughly coincides with the first minimum in $S(q)$. In the future we hope to obtain more reliable data. At present, however, these are the only data extant for the structure factors of the metastable and glassy phases and are, we think, reliable enough for a preliminary analysis.

The experimental values of $S(q)$, obtained in this way, are shown in Figs. 1–4 for a range of volume fractions. The experimental uncertainties mentioned above and the limited range of scattering vectors over which $S(q)$ can be measured preclude the computation of $g(r)$ by means of the inverse of Eq. (3). So we rely on the hard-sphere model (see below) to provide further interpretation of the experimental data.

III. STRUCTURE OF THE HARD-SPHERE SYSTEM

A variety of statistical mechanical techniques has been used to map out the phase diagram of a system of hard spheres;[13] a schematic representation of this phase diagram is shown in Fig. 5. For $\phi < \phi_F$ the system exists in a thermodynamic equilibrium fluid phase with significant short range but no long-range spatial correlation among the particles. The equilibrium state for $\phi > \phi_m$ is an ordered or crystalline arrangement of particles in hexagonally packed planes. The structure indicated by molecular-dynamics (MD) studies is face-centered cubic (fcc) whereas the crystal phase of the dispersions, discussed in Sec. II, displays a strongly faulted stacking of the hexagonal planes,[14] i.e., a combination of fcc and hexagonal close packing (hcp). It is this faulty stacking that gives rise to the spectacular diffraction colours in these dispersions and precious opal.[5,15] For volume fractions between ϕ_F and ϕ_m the disordered and crystal phases coexist in equilibrium.[5]

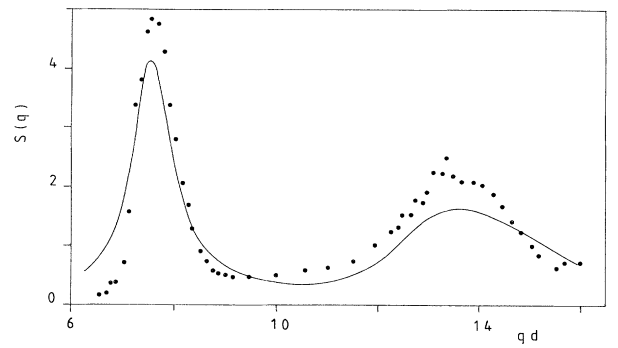

FIG. 4. Same as for Fig. 1 but $\rho^* = 1.18$.

It has recently been shown that it is possible, on a time scale accessible to molecular-dynamics computer simulation, to compress a hard-sphere fluid to volume fractions beyond ϕ_m at a rate where crystallization is prevented.[13] For $\phi > \phi_m$ the particles in the metastable state so produced may still diffuse over appreciable distances (in comparison with the interparticle spacing), so that in time the system will tend to go to the equilibrium crystal phase.[13] However, continued compression before any appreciable equilibration, or relaxation of the structure, will produce an amorphous state at a volume fraction ϕ_g for which the structural relaxation time is (essentially) infinite and long-ranged particle diffusion has ceased, i.e., a glass.[8,13] Using several criteria, such as the vanishing particle diffusivity, an estimate of the location of this hard-sphere glass transition is $\phi_g = 0.568$.[13]

The properties of the glass state are dependent on the method of preparation and the criteria used for locating the glass transition. This is borne out by the result of Woodcock's work that the maximum volume fraction $\phi_{\max}$ obtained for the amorphous state (glass) depends on the rate of compression of fluid initially in equilibrium. Very rapid compression yields $\phi_{\max} = 0.637$ which corresponds to the limit obtained by Bernal in experiments

with steel ball bearings. Slower compression, but still preventing crystallization, gives $\phi_{max}=0.654$.[16]

The radial distribution function is known in the form of an excellent algebraic fit to computer simulation results for the equilibrium hard-sphere fluid[17] and crystal.[18] Corresponding empirical results or tested theoretical predictions for the metastable fluid and glass are presently not available. We have, therefore, carried out several MD computer calculations on hard spheres in order to obtain $g(r)$ and $S(q)$ for the metastable and glass states to investigate their structure more fully than in previous work[13] and also to compare with the experimental results discussed above.

The MD calculations performed here use the algorithm of Alder and Wainwright,[19] and the compression or densification scheme originally suggested by Woodcock[20] which involves expansion of the diameters of the particles, every ΔN collision, until the two closest spheres just touch. $N=500$ spheres at a volume fraction $\phi=0.47$ were placed on an fcc lattice subject to the usual periodic boundary conditions. The MD computation was commenced allowing this system to melt and attain equilibrium from whence the computation was continued and $g(r)$ and the compressibility factor pV/NkT calculated until they agreed with the results of Barker and Henderson[21] for the equilibrium fluid (see Table I). From the final (equilibrium) particle configuration a compression sequence, with $\Delta N=10$ collisions, was commenced in order to simulate a rapidly compressed fluid. The compression was interrupted at various volume fractions (or densities) and the MD computation allowed to proceed (at this den-

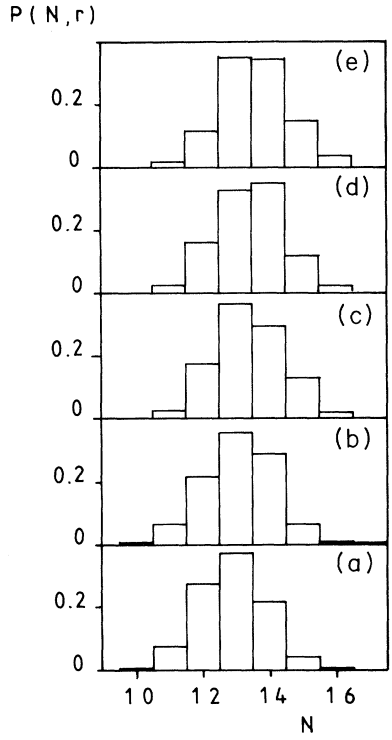

FIG. 6. Nearest-neighbor coordination numbers $P(N,r)$ vs N for rapidity quenched states, N=coordination number, $r=1.45d$. (a) $\rho^*=1.044$, (b) $\rho^*=1.10$, (c) $\rho^*=1.14$, (d) $\rho^*=1.155$, (e) $\rho^*=1.18$.

TABLE I. Compressibility factors, $Z=pV/NkT$ for the hard-sphere states generated in this study. The free-volume approximations are included to illustrate the fact that they accurately describe the behavior of the two extreme amorphous solids, i.e., those produced by rapid and slow compression.

ρ^*	Rapid compression	Slow compression	"Equilibrium"	Free-volume approximation[a,b]	
0.90	10.7		10.7[c]	10.5	9.6
1.044	19.9	19.1	18.5[d]	20.2	17.0
1.10	28.8	25.4[e]	23.3[d]	30.5	23.6
	(28.1[f])	17.7[g]			
		(13.6[h])			
1.14[i]	43.6		31.1	47.1	32.4
1.155	52.5		36.0	59.0	37.5
1.180	89.3		50.0	100.0	50.7

[a] $pv/NkT=[1-(\rho/\rho_B)^{1/3}]^{-1}$, $\rho_B=1.2158$.
[b] $pv/NkT=[1-(\rho/\rho_a^0)^{1/3}]^{-1}$, $\rho_a^0=1.2525$.
[c] Reference 21.
[d] Reference 13.
[e] Glass, this work.
[f] Reference 20.
[g] Imperfect crystal, this work.
[h] fcc crystal, K. R. Hall, J. Chem. Phys. **57**, 2252 (1972).
[i] $\rho^*=\rho d^3$.

sity) until stable values for $g(r)$, pV/NkT, and several other properties (discussed below) were obtained. A second set of computations, discussed in Sec. V, was performed at a much lower rate of compression.

Further insight to the structure of the system is provided by the probability distribution $P(n,r)$ of the nearest-neighbor coordination number n, which we calculated at the arbitrarily chosen value of $r=1.45$ (expressed in units of the particle diameter) corresponding roughly with the first coordination shell. As can be seen from Fig. 6 there is, as for the glassy state of Lennard-Jones atoms,[22] a wide distribution of n. This contrasts the stable crystal for which n is fixed. Although not shown here, similar results were obtained for the second and third coordination shells.

The second peak of $g(r)$ (Figs. 7 and 8) shows the splitting characteristic of the amorphous state of systems of particle interacting with hard potentials.[23] From an analysis of close-packed amorphous structures of hard spheres it has been shown that the longer of the two preferred distances, which causes this splitting, corresponds to a collinear arrangement of triplets of particles while the shorter arises from the distance of closest approach of a second nearest neighbor across an intervening pair of particles in the nearest-neighbor shell.[23] Subsequent peaks in $g(r)$, on the other hand, appear very similar to those of the (less dense) equilibrium fluid except that significant structure extends to larger distances.

In order to compare the structure obtained by the MD computations with experimental data we must compute $S(q)$. One can do this directly from the MD generated configurations but this turns out to be too slowly convergent and, also, can only be done for a few discrete values of q.[24] Thus, we have computed $S(q)$ from $g(r)$ by using Eq. (3). In order to get accurate results by this method one needs to carefully extrapolate $g(r)$ beyond $r=L/2$ where L is the length of the cubic cell containing the N particles, since the MD method only gives $g(r)$ in the range $0<r<L/2$.

As in previously published work[24] we have chosen to extrapolate $g(r)$ with the function:

$$f(r)=1+A\exp(-Br)\cos(Cr+D)/r\ , \tag{5}$$

where the parameters A, B, C, and D are obtained by fitting $f(r)$ to the larger r portion of the MD radial distribution function. This method has been shown to be of sufficient accuracy by comparison with directly calculated values of $S(q)$ calculated from very long computer runs at some selected densities for both soft- and hard-sphere systems.[24] Its accuracy was further checked for very dense amorphous states by the following scheme. The Percus-Yevick (PY) theory for hard spheres provides analytical expressions for both $g(r)$ and $S(q)$,[25] thus a

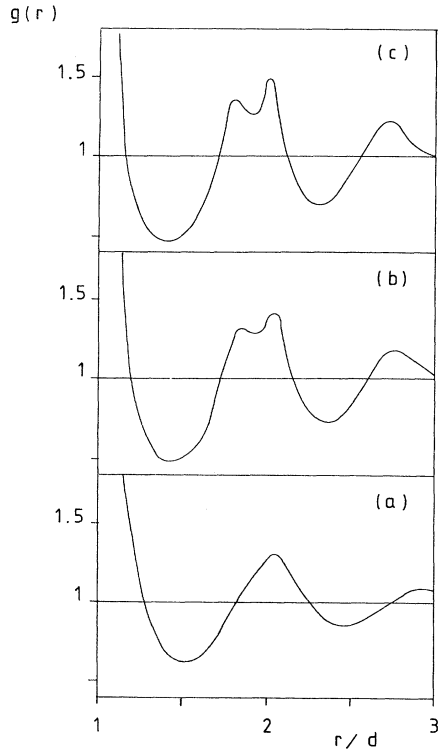

FIG. 7. Second and third peaks of $g(r)$ for rapidly compressed fluid and glass. (a) $\rho^*=0.90$, (b) $\rho^*=1.044$, (c) $\rho^*=1.10$.

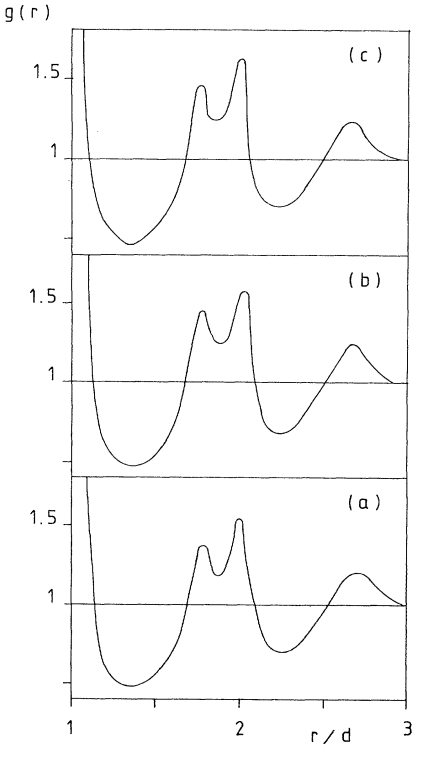

FIG. 8. Same as for Fig. 7 but (a) $\rho^*=1.14$, (b) $\rho^*=1.155$, (c) $\rho^*=1.18$.

comparison of this analytical $S(q)$ with that generated numerically by truncating the PY $g(r)$ at $L/2$, extrapolating and numerically integrating by the above procedure gives a direct measure of the accuracy of our values of $S(q)$. This direct comparison reveals the following differences: (i) for the height of the first maximum a difference of about 1% at $\phi=\phi_F$ and about 7% at $\phi=0.61$, (ii) for subsequent minima and maxima differences of about 1%, and (iii) differences of about 1% for the positions of the maxima and minima. In fact as the features of $g(r)$ (e.g., peak heights) are overestimated by the PY approximation then the above comparison will give an upper bound to the errors in our method.

IV. COMPARISON OF EXPERIMENT AND MOLECULAR DYNAMICS

Figures 1–4 show a comparison of the structure factors calculated by the MD method and measured by light scattering for the equilibrium fluid phase at freezing ($\phi=\phi_F$) and for three volume fractions in the amorphous phase. Considering the uncertainties in the experimental data, discussed above, the agreement between the two sets of results is reasonable. Several points emerge from Figs. 1–4.

(i) Except for the primary maximum for the fluid at freezing, the positions of the minima and maxima are in good agreement.

(ii) The first minimum is quite broad and flat.

(iii) The height of the first peak in $S(q)$ does not increase very sharply with increasing ϕ, in contrast with the predictions of the Percus-Yevick theory for hard spheres (see Table II).

(iv) Within the accuracy of the data neither experiment nor MD suggest a split of the second maximum of $S(q)$. This is at variance with recent theoretical work.[26]

(v) The ratios of the magnitudes of the first and second maxima as well as maxima to minimum ratios also agree quite well (see Table II). One must be cautious, however, in making too much of quantitative comparisons in the region of the first minimum and second maximum. This is because $S(q)$ was obtained by dividing $I(q)$ by $P(q)$ and in these regions $P(q)$ is very small and quite uncertain in magnitude.

The most severe differences between experiment and the MD results occur in the vicinity of the main peak of $S(q)$ (Figs. 1–4). To appreciate these discrepancies it must be noted that the PMMA particles in the refractive index matching liquid can be regarded optically as homogeneous Rayleigh Gans-Debye scatterers, for which the form factor $P(q)$ decreases most steeply with q around the position of the maximum $q_{\max}$ in $S(q)$. Thus, small errors in the measurements of either $I(q)$ or $I_0(q)$ may translate into more significant uncertainties in $S(q)$. In addition, errors in q, resulting from the refraction corrections for the sample cells of the square cross section used in these experiments, may be significant especially in the forward angles ($\theta<25°$).

V. EFFECT OF THE RATE OF COMPRESSION

In order to investigate the effects of the rate of compression on the structure of the hard-sphere metastable system we performed a MD computation commencing from the equilibrium fluid at $\phi=0.47$ with a compression step every $\Delta N=2000$ collisions. Having reached the volume fraction of $\phi=0.547$ it was held fixed and the MD computation was allowed to proceed for 2×10^6 collisions. The pressure calculated for this state is marginally larger than Woodcock's[13] so-called "equilibrium metastable fluid" at the same volume fraction (see Table I). The slow compression ($\Delta N=2000$) was then continued to $\phi=0.563$ followed by a rapid compression ($\Delta N=10$) to $\phi=0.576$. As found by Woodcock,[13] the rapid compression was necessary at this stage to avoid crystallization. Table I shows that the pressure [and therefore also the height of the first peak in $g(r)$] of this glass ($\phi=0.576$) obtained with several slow compression stages is significantly lower than that for the rapidly compressed glass although still slightly greater than Woodcock's[13] "equilibrium glass." The lowering of the pressure of the glass at $\phi=0.576$ is simply a reflection of the extra structural relaxation that can be accommodated during the slower compression. This suggestion is supported by the fact that the pressure of the equilibrium crystal, and an imperfect crystal (see below), are very much lower again (see Table I). Also a comparison of the radial distribution functions of the ($\phi=0.576$) glasses obtained by slow and rapid compression (Fig. 9) shows that the slow compression yields the more compact structure; an increase in the height of the first component of the split second peak relative to the first component, and more strongly depleted minima are observed for the slower compression rate. Similar features have previously been observed for glasses of Lennard-Jones atoms[27] and also for a hard sphere glass[13] at $\phi=0.628$. These differences

TABLE II. Comparison of Perkus-Yevick, molecular-dynamics, and experimental estimates of certain features of $S(q)$.

	$S(q)_{\max_1}/S(q)_{\min}$			$S(q)_{\max_1}/S(q)_{\max_2}$			$S(q)_{\max_2}/S(q)_{\min}$		
ρ^*	PY	MD	Expt.	PY	MD	Expt.	PY	MD	Expt.
0.943	5.7	5.2	4.7	2.2	2.1	1.7	2.6	2.5	2.7
1.10	14.1	9.0	8.4	3.0	2.5	2.1	4.7	3.5	4.0
		−10.3			−2.8			−3.7	
1.14	18.7	9.9	8.5	3.3	2.5	2.1	5.7	4.0	4.1
			−9.8			−2.2			−4.6
1.18	26.3	11.7	9.7	3.5	2.5	1.9	7.5	4.7	5.0

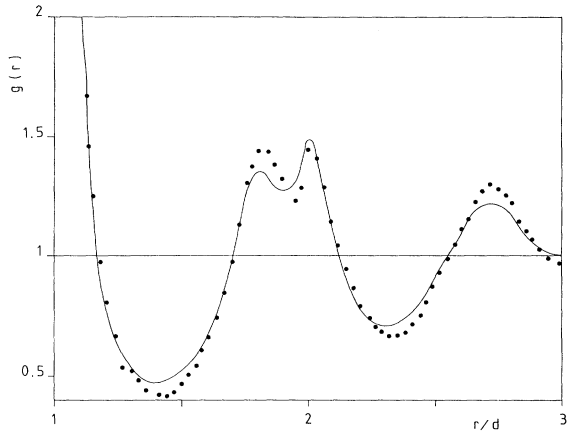

FIG. 9. $g(r)$ showing the effect of the rate of compression on the second and third peaks, showing results for rapid compression (——) and slow compression (●).

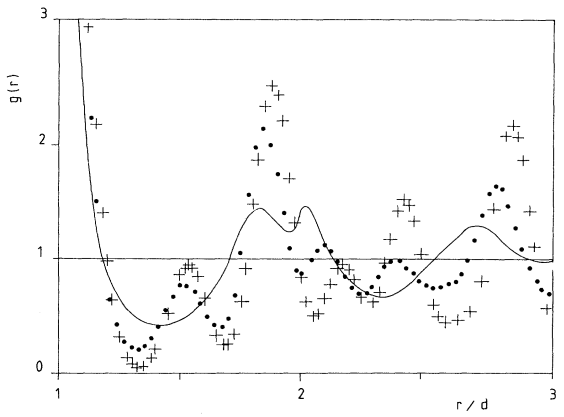

FIG. 11. Comparison of $g(r)$ for the slowly compressed glass (——), the imperfect crystal (●), and the perfect crystal (+).

in $g(r)$ of glasses obtained by different compression rates are, surprisingly, virtually absent in the structure factor, either measured or calculated. Clearly the Fourier transformation of $g(r)$ smears at any differences and only results in a slightly higher primary maximum in $S(q)$ in both cases (see Figs. 3 and 10).

Another interesting feature observed in the dispersions in the volume fraction range $\phi_F < \phi < \phi_g$ is that they crystallize homogeneously,[5] i.e., the crystallization nuclei are uniformly distributed throughout the sample volume. After an equilibration period of a few days dispersions in the volume fraction range $\phi_F < \phi < \phi_m$ are clearly separated into a crystalline phase, at volume fraction ϕ_m and a disordered phase at volume fraction ϕ_F. For $\phi_m < \phi < \phi_g$, the crystalline phase occupies the whole volume. Except for $\phi \gtrsim \phi_g$, where large crystals nucleated heterogeneously at the cell walls are observed, the crystalline phases consists of small (diameter approximately 50 μm) randomly oriented crystals.[5] A detailed diffraction study suggests that these crystals consists of a faulted stacking of hexagonally packed layers of particles, i.e., a mixture of hcp and fcc structures.[7,14]

Crystallization from the metastable phase can also be obtained in the computer simulations by slow compression ($\Delta N = 2000$) from $\phi = 0.47$ to $\phi = 0.576$. If the MD calculation is continued at $\phi = 0.576$ the onset of crystallization is signaled by a sudden drop in pressure. That this crystal is imperfect is indicated not only by its pressure excess over the equilibrium fcc crystal (see Table I) but also explicitly in Fig. 11 where its radial distribution function is compared with that for the perfect crystal. The latter was obtained from the algebraic expression of Weis and Kincaid.[18]

The experimental and theoretical structure factors calculated on the basis of an isotropic system of the crystalline phases at $\phi = 0.576$, obtained in both cases by crystallization of the disordered or fluid metastable phase, are shown in Fig. 12.

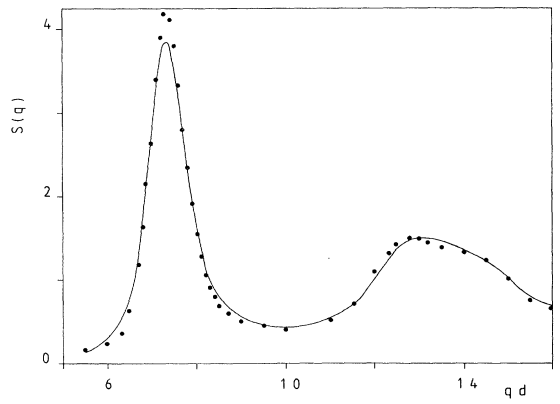

FIG. 10. Same as for Fig. 9 except $S(q)$ instead of $g(r)$.

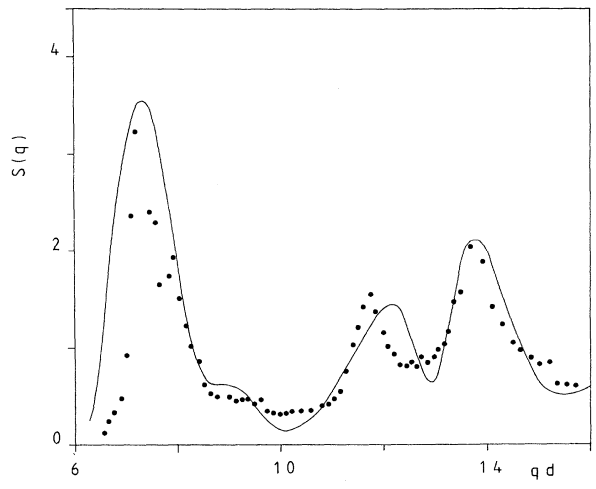

FIG. 12. Comparison of $S(q)$ for the imperfect crystal from MD (——) and experiment (●). $\rho^* = 1.10$.

VI. CONCLUSIONS

In this paper we have reported structure factors $S(q)$ and their interpretation in terms of the hard-sphere system for a well-defined model sterically stabilized colloidal system. Hopefully, studies of this type will lead to as much understanding of the state of aggregation and properties of these systems as aqueous suspensions of polymer lattices have for charge stabilized systems. This system shows fluid, crystal and glasslike structure and also coexistence between fluid and crystal structures.

These phases are important from several points of view.

(i) Glassy phases may be used to explain and model shear thickening behavior.

(ii) Ordered colloids are useful for modeling systems with a yield value.

(iii) They are important for ceramic processing (this is especially relevant as the polymer used here may be used to stabilize oxide particles).

(iv) They may be used to study glass formation and dynamics.

(v) They provide useful systems in which to observe both homogeneous and heterogeneous crystallization.

To continue on point (iii), although random close-packed states may be of lower volume fraction ($\phi=0.64$) than regular (hexagonal) close packing ($\phi=0.74$), the latter tends, on a macroscopic scale, to be polycrystalline.[5] A ceramic produced from this state may possess mechanical weaknesses, possibly exacerbated by sintering, in the vicinity of the grain boundaries. Not only is the random arrangement of particles more likely to be free from such macroscopic faults, but it is more easily and quickly produced than the (imperfect) crystalline phase.

Finally, this study complements that of Woodcock on the thermodynamic properties, formation, and transport properties of the hard-sphere glass in that we have provided some insight into the structure of these systems as a function of density and rate of formation.

[1]P. Calvert, Nature (London) **317**, 204 (1985).
[2]E. A. Barringer and H. K. Bowen, Comm. Am. Ceram. Soc., Dec., C-199 (1982).
[3]R. J. R. Cairns, W. van Megen, and R. H. Ottewill, J. Colloid Interface Sci. **79**, 511 (1981).
[4]L. Antl, J. W. Goodwin, R. D. Hill, R. H. Ottewill, S. M. Owens, S. Papworth, and J. A. Waters, Colloids Surf. **17**, 67 (1986).
[5]P. N. Pusey and W. van Megen, Nature (London) **320**, 340 (1986).
[6]P. N. Pusey and W. van Megen, J. Phys. (Paris) **44**, 258 (1983).
[7]P. N. Pusey and W. van Megen, in *Physics of Complex and Supramolecular Fluids,* edited by S. A. Safran and N. A. Clark (Wiley, New York, 1987).
[8]P. N. Pusey and W. van Megen, Phys. Rev. Lett. **59**, 2083 (1987).
[9]W. van Megen, S. M. Underwood, and I. Snook, J. Chem. Phys. **85**, 4065 (1986).
[10]J. Jackle, Rep. Prog. Phys. **49**, 171 (1986).
[11]W. G. Hoover and F. M. Ree, J. Chem. Phys. **49**, 3609 (1968).
[12]J. P. Hansen and I. R. McDonald, *Theory of Simple Liquids,* (Academic, New York, 1976).
[13]L. V. Woodcock, Ann. N.Y. Acad. Sci. **37**, 274 (1981).
[14]P. N. Pusey, W. van Megen, P. Bartlett, B. J. Ackerson, J. G. Rarity, and S. M. Underwood, Phys. Rev. Lett. **63**, 2753 (1989).
[15]P. J. Darragh, A. J. Gaskin, and J. V. Sanders, Sci. Am., April, 84 (1976).
[16]J. D. Bernal and J. Mason, Nature **188**, 910 (1960); J. D. Bernal, Proc. R. Soc. London, Ser. A **280**, 299 (1964).
[17]L. Verlet and J. J. Weis, Phys. Rev. A **5**, 939 (1972).
[18]J. M. Kincaid and J. J. Weis, Mol. Phys. **34**, 931 (1977).
[19]B. J. Adler and T. E. Wainwright, J. Chem. Phys. **33**, 1439 (1960).
[20]L. V. Woodcock, J. Chem. Soc. Faraday Trans. 2 **74**, 1667 (1976).
[21]J. A. Barker and D. Henderson, Mol. Phys. **21**, 187 (1971).
[22]C. A. Angell, J. M. R. Clarke, and L. V. Woodcock, Adv. Chem. Phys. **48**, 397 (1981).
[23]G. S. Cargill, Solid State Phys. **30**, 227 (1975); M. R. Hoare, J. Non-Cryst. Solids **31**, 227 (1975).
[24]K. Gaylor, I. Snook, and W. van Megen, J. Chem. Phys. **75**, 1682 (1981); W. van Megen, I. Snook, and P. N. Pusey, *ibid.* **78**, 931 (1983).
[25]N. W. Ashcroft and J. Lekner, Phys. Rev. **148**, 83 (1966).
[26]S. Sachdev and D. R. Nelson, Phys. Rev. Lett. **53**, 1947 (1984).
[27]J. M. R. Clarke, J. Chem. Soc. Faraday Trans. 2, **75**, 1371 (1979).